

Spectroscopic Analysis and Geometry Assignment of the Minimum Energy Conformations of 2-Phenoxypyridines and Diphenyl Ethers

Bunji UNO,* Toshio KAWAKITA, Kenji KANO,
Kiyoshi EZUMI,[†] and Tanekazu KUBOTA
Gifu Pharmaceutical University, Mitahora-higashi, Gifu 502
[†]Shionogi Research Laboratory, Shionogi and Co., Ltd.,
Fukushima-ku, Osaka 553
(Received September 4, 1991)

The conformational preferences of 2-phenoxypyridines and diphenyl ethers were determined by minimum-energy optimization using the method of ab initio molecular orbital calculations with STO-3G basis sets, and by spectral measurements and their analyses based on CNDO/S-CI calculations. The *o,o*-disubstituents of the methyl groups to diphenyl ether and 2-phenoxypyridine, i.e., 1,3-dimethyl-2-phenoxybenzene and 2-(2,6-xylyloxy)pyridine, respectively, prefer a symmetric skew conformation. The conformation of unsubstituted diphenyl ether (**1a**) is nonrigid with a dihedral angle, about 90°, of two phenyl rings at room temperature. Spectral observations at 77 K have provided evidence for this conclusion. On the other hand, 2-phenoxypyridine (**2a**) has been found to possess sufficient internal barriers to stabilize the two aromatic rings in a skew form. The weak nuclear repulsion, compared with that in **1a**, would mainly contribute to stability in the skew form. The characteristic ¹L_a band observed for **2a** is attributed to the configuration interaction of the n-π* excited state to the ¹L_a states in the skew form.

It is well known that phenoxypyridines and diphenyl ethers are of biological importance as basic skeletons of thyroid hormones and drugs. The conformational preferences of phenoxypyridines and diphenyl ethers are of great interest in chemistry both as typical compounds having critical oxygen aromatic properties, and concerning the structure-activity relationships of thyroid hormones.^{1–4)} The conformations of this kind of compound are traditionally classified into four groups (Fig. 1) by taking 2-phenoxypyridine (**2a**) as an example. The conformation of diphenyl ether (**1a**) was first discussed by Higashi and Smyth;⁵⁾ there have subsequently been many reports concerning this subject.^{1–19)}

Robertson and co-workers have discussed the effects of two *o*-substituents introduced to a phenyl ring of **1a**, and determined the preferable conformations of the *o,o*-disubstituted diphenyl ethers as a skew form in crystals.^{6,7)} Lehmann has proposed that the *o*-monosubstituted derivatives preferentially adopt twist conformations as a result of the balance between the conjugative tendency toward coplanarity and the steric hindrance.⁸⁾

A variety of experimental and theoretical approaches have suggested that **1a** prefers a twist form in which θ_1 and θ_2 lie in the vicinity of 25–50° with some exceptions.^{9–12)} The twist form, however, has not yet been

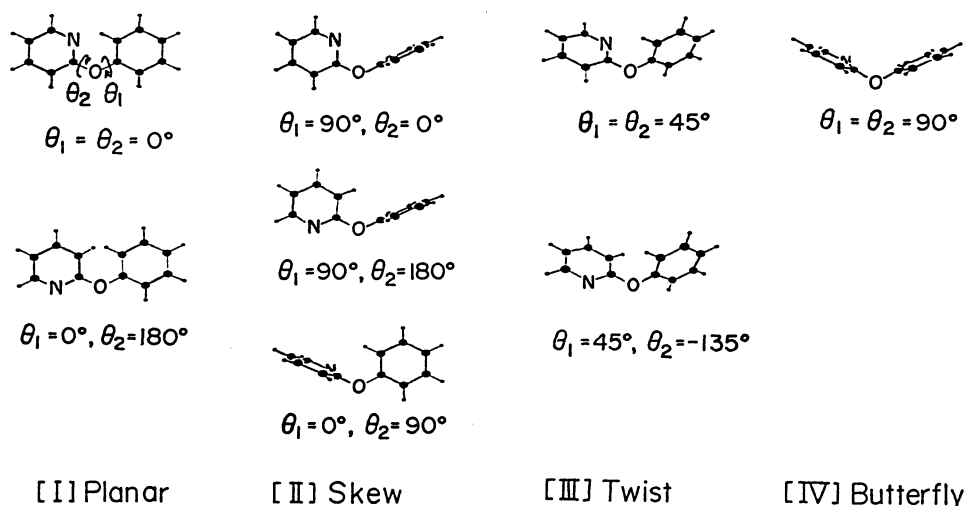


Fig. 1. Stereoscopic view of typical conformations for 2-phenoxypyridine (**2a**). θ_1 and θ_2 denote the angles of twist about the C–O bonds, respectively. They are defined as zero when the phenyl and pyridyl rings are in the COC plane. The increases in θ_1 and θ_2 cause clockwise rotations of the phenyl and pyridyl rings around their O–C bonds, respectively.

well justified. Recently, a great deal of attention has been focused on the internal motion of **1a**,^{3,11,13)} since the barrier concerning internal rotation around the C–O bonds on **1a** is suggested to be as low as 2.44 kcal mol^{−1},¹²⁾ and the enthalpy of activation is also 2.4 kcal mol^{−1}, as estimated in a polystyrene matrix.¹⁴⁾ Ab initio and semiempirical C-INDO approaches to the internal barrier in **1a** suggest the so-called one-ring flip mechanism.^{13,15)} It has therefore been required to experimentally clarify whether **1a** adopts a nonrigid conformation or not.

On the other hand, only a few theoretical and experimental investigations have been carried out concerning the preferable conformation of **2a**, which involves critical torsion angles with regard to conjugation between the phenyl and pyridyl rings through the bridging oxygen atom. There seems to be a large difference in the nuclear repulsion between **2a** and **1a**, though the number of π -electrons is identical. It is therefore of interest and importance in structural chemistry to understand what difference occurs in the conformations of **2a** and **1a** brought about by the balance between electronic stabilization (conjugation) and steric repulsion.

In this report we discuss the preferable conformations of **1a** and **2a** in terms of the geometry assignment of the minimum energy, as well as spectroscopic measurements and their analyses using the method of CNDO/S-CI

calculations.

Experimental

Chemicals and Solvents. The samples used here were **1a**, 1,3-dimethyl-2-phenoxybenzene (**1b**), anisole (**1c**), **2a**, 2-(2,6-xylyloxy)pyridine (**2b**), 2-methoxypyridine (**2c**), toluene (**3a**), *m*-xylene (**3b**), as illustrated in Fig. 2. Compounds **1a**, **1c**, **2c**, and **3a–b** were commercially available (Wako Chemical Co. or Aldrich Chemical Co.) and were repeatedly distilled under reduced pressure before use. Samples **1b** and **2a–b** were synthesized according to the method of Ullman.^{20–22)} Upon recrystallization from petroleum ether purified **2a** was obtained (mp 46.0°C). The purification of **1b** and **2b** was achieved by preparative thin-layer chromatography and distillation under reduced pressure, respectively; they were then recrystallized from petroleum ether (mp 58.0–59.0°C for **1b** and 54.0–55.0°C for **2b**). The structure and purity of all the samples were checked by thin-layer chromatography, elemental analyses and mass spectrometry. Good agreements were obtained between the experimental and calculated values in the elemental analyses.

The solvents used for the spectral measurements were heptane and EPA solution (ether:2-methylpentane:ethyl alcohol=5:5:2) of spectrograde purity. These were sufficiently dried over CaH₂, except for ethyl alcohol, of which desiccation was achieved using CaO; it was then carefully rectified. 2-Methylpentane was further purified through a column packed in the order unhydrous sodium sulfate, aluminium oxide and silicon dioxide.

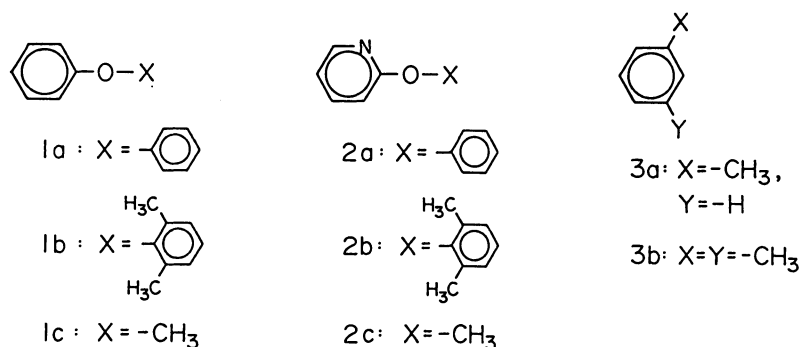


Fig. 2. Molecules employed in this study.

Table 1. Observed Spectral Data at Room Temperature and 77 K

Compound	at Room temperature ^{a,b)}						at 77 K ^{a,c)}					
	¹ L _a band			¹ L _b band			¹ L _a band			¹ L _b band		
	$\lambda_{\text{max}}/\text{nm}$	$E/\text{eV}^{d)}$	ϵ_{max}	$\lambda_{\text{max}}/\text{nm}$	$E/\text{eV}^{d)}$	ϵ_{max}	$\lambda_{\text{max}}/\text{nm}$	$E/\text{eV}^{d)}$	ϵ_{max}	$\lambda_{\text{max}}/\text{nm}$	$E/\text{eV}^{d)}$	ϵ_{max}
1a	226.0	5.49	9710	272.0	4.56	1910	229.0	5.41	15400	272.5	4.55	3200
1b	217.5 ^{e)}	5.70	16800	271.2	4.57	2120	217.5 ^{e)}	5.70	18800	271.0	4.58	3000
1c	220.0	5.64	7430	271.3	4.57	2020						
2a	220.0	5.64	11600	272.0	4.56	3510	220.0	5.64	15200	272.5	4.55	4150
2b	213.5	5.81	20500	273.0	4.54	3830	213.5	5.81	23200	272.0	4.56	4420
2c	214.5	5.78	8140	273.2	4.54	3890						
3a	207.5	5.98	8250	262.2	4.73	261						
3b	211.5	5.86	13400	265.7	4.67	274						

a) Values at the maximum intensity. b) Values in heptane. c) Values in an EPA solvent. d) The transition energy in eV unit. e) The values are for the shoulder band.

Spectral Measurements. The absorption spectra of all the samples were recorded with a Hitachi spectrophotometer (Model 323) at room temperature, unless otherwise stated. The spectra at 77 K were measured for **1a**—**b** and **2a**—**b** in an EPA solvent using a Dewar-type cell. The recorded absorbance was multiplied by 0.798 in order to correct for any concentration change arising from contraction of the sample solution upon cooling. All of the operations at 77 K were carried out under an N₂ atmosphere. The observed spectral data are listed in Table I.

Molecular Orbital (MO) Calculations. Ab initio MO calculations were carried out in order to analyze the minimum-energy conformations of **1a**—**b** and **2a** with STO-3G minimum basis sets, since split-valence basis sets and polarization functions could not be employed, due to a restriction in the program used. This computed structure, however, can serve as a basis for full energy minimization calculations with larger basis sets, as yet unperformed. The molecular geometries were determined by referring to the results of X-ray crystallographic analyses for methyl 4-mesityloxy-3-nitrobenzoate and 2-(2,6-dinitrophenoxy)-*t*-butylbenzene⁶⁾ with the following minor modification. A regular hexagon of 1.385 Å was assumed for the aromatic rings, in which the C—H distance was fixed at 1.084 Å. A fixed length of 1.390 Å was adopted for both the C—O bonds. The so-called standard structural parameters were used for the methyl group. The C—O—C angle was optimized for each of the typical conformations of **1a** and **2a** shown in Fig. 1. These optimizations yielded values of 115–121° for all the conformations of **1a** and **2a**. A C—O—C angle of 120° was, thus, assumed. The same value was also found in X-ray diffraction studies⁶⁾ as well as in recent calculations of **1a**.^{11,13)} The conformational energies were computed in the counter rotations to each other (θ_1 and θ_2 in Fig. 1) at every 15° angle around the two C—O bonds.

In order to interpret the experimental absorption spectra, CNDO/S-CI calculations were carried out. The parameters necessary for the calculations were taken from the literature of Jaffé's group as well as that of others.²³⁾ Two-center repulsion integrals were evaluated using Nishimoto–Mataga's equation.²⁴⁾ Only the one-electron transition was taken into account for calculations of the configuration interaction (CI).

Results and Discussion

Minimum Energy Conformations. Figure 3 shows the relative total energies calculated for **1a** at 15° intervals of θ_1 and θ_2 . Compound **1a** was found to have low conformational energies over the range θ_1 and θ_2 , satisfying the relation $\theta_1 + \theta_2 \approx 90^\circ$, where the two bridged phenyl rings form a dihedral angle of almost 90°. Although the twist form ($\theta_1 = \theta_2 = 45^\circ$) is the minimum, the energy is low by only 0.2 kcal mol⁻¹, compared with that of the skew form, which is the maximum among them. This supports the so-called one-ring flip mechanism^{16,17)} for the internal motion of **1a**, proposed by Schaefer et al.¹³⁾ Recent studies concerning the molecular mechanics (MM2) suggest a conformation of the two phenyl rings that is similar to the above.¹⁸⁾ The calculations for **1a** also indicate that the change in the nuclear repulsion and electronic energies with a conformational change of the twist to skew forms is quite large, but just reverse in the energy change direction

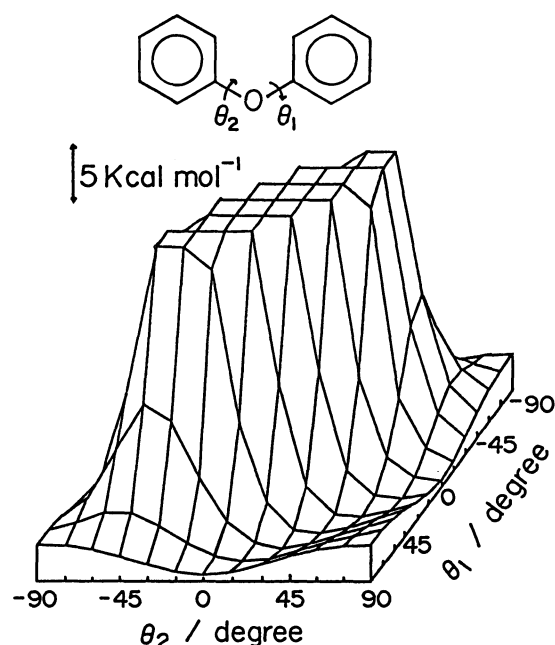


Fig. 3. STO-3G total energies of **1a** at 15° intervals of the θ_1 and θ_2 angles.

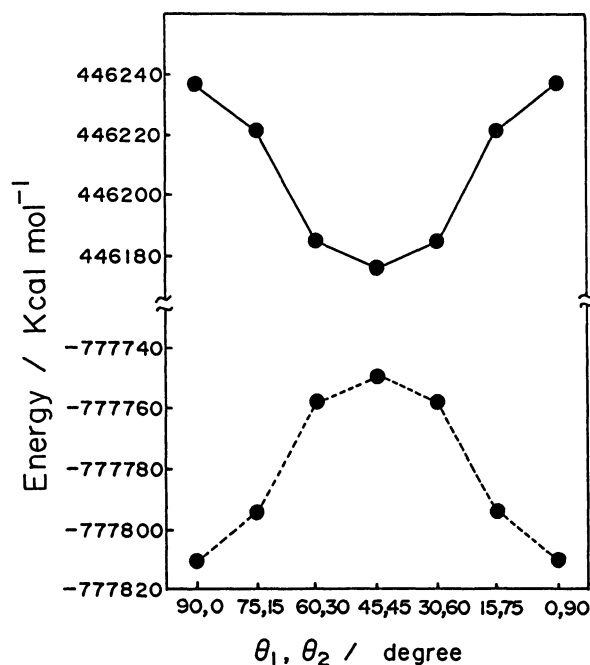


Fig. 4. Nuclear repulsion (solid line) and electronic (dotted line) energies of **1a** pertinent to changes in the θ_1 and θ_2 angles from 0° to 90° and from 90° to 0°, respectively.

(Fig. 4). The total energies are therefore almost constant in the conformational alteration within the rotation angles $\theta_1 + \theta_2 \approx 90^\circ$. The fact that the electronic energy is remarkably stabilized in the skew form may be due to the conjugation of the lone-pair π -electrons upon the oxygen atom with one of the phenyl rings.^{25–28)} On

the contrary, the nuclear repulsion energy is remarkably larger in the skew form of **1a**, rather than that in the twist form (see Fig. 4). This would undoubtedly arise from the steric hindrance between the *ortho* hydrogen atom inside the COC angle and the opposite phenyl ring. From the above point of view it is not certain whether **1a** would have the necessary stable skew conformation to reduce the steric repulsion, as concluded in the classic studies.¹⁹⁾ Figure 5 shows the relative energy

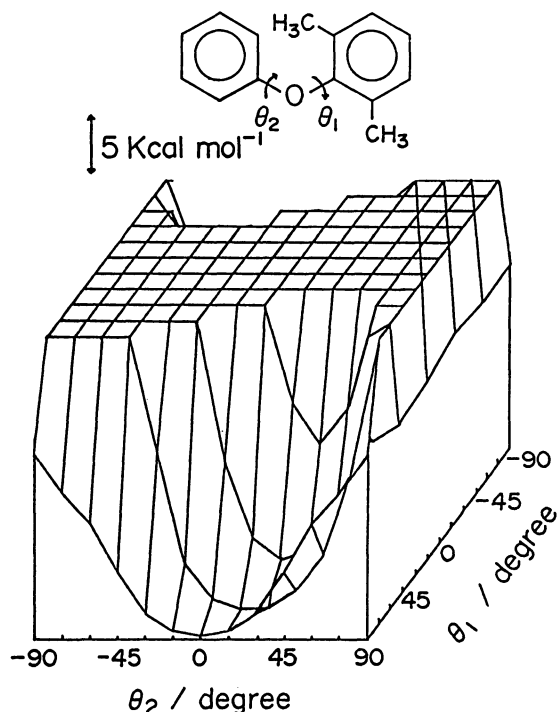


Fig. 5. STO-3G total energies of **1b** at 15° interval of the θ_1 and θ_2 angles.

of **1b** as a function of θ_1 and θ_2 . As expected, **1b** predominantly occupies a symmetric skew conformation ($\theta_1=90^\circ$, $\theta_2=0^\circ$) because of the steric hindrance caused by the bulky methyl substituents at the *o*-positions.⁶⁾ Our calculations show that the electronic energy as well as the nuclear repulsion contributes to the stable skew form of **1b**.

The conformational energy map of **2a** (Fig. 6) looks somewhat different from that of **1a**. The change in θ_1 and θ_2 from 90° to 0° and from 0° to 90° , respectively, gives rise to a ravine on the energy map with an energy gradient in the direction of a skew form of $\theta_1=90^\circ$ and $\theta_2=0^\circ$. Therefore, the minimum energy occurs at the skew conformation wherein the nitrogen atom lies inside the COC angle and the oxygen π -electrons conjugate with the pyridyl ring ($\theta_1=90^\circ$, $\theta_2=0^\circ$). Strictly speaking, the minimum-energy conformation of **2a** is observed at $\theta_1=75^\circ$ and $\theta_2=0^\circ$; it is thus classified as a skew type,⁶⁾ the energy being stable by only 0.1 kcal mol⁻¹, compared with that at $\theta_1=90^\circ$ and $\theta_2=0^\circ$. It should be noted that in the skew form of **2a** the nuclear repulsion energy is relatively less than that of **1a**. Our present STO-3G calculations reveal that **2a** possesses sufficient internal barriers with regard to rotation around the two C–O bonds in order to maintain the skew conformation.

Electronic Spectra of Diphenyl Ethers. Figure 7 shows the absorption spectra of **1a** and **1b**. The composite spectra of **3a** and **1c**, as well as those of **3b** and **1c**, being abbreviated (**3a+1c**) and (**3b+1c**), respectively, are also illustrated. All of the spectra are similar to each other, and are assigned to the 1L_b and 1L_a bands²⁹⁾ in the order from the long-wavelength side. The characteristics of the 1L_a band of these compounds reflect the degree of conjugation.²⁹⁾ If both π -electron systems of the bridged aromatic rings cannot interact with each

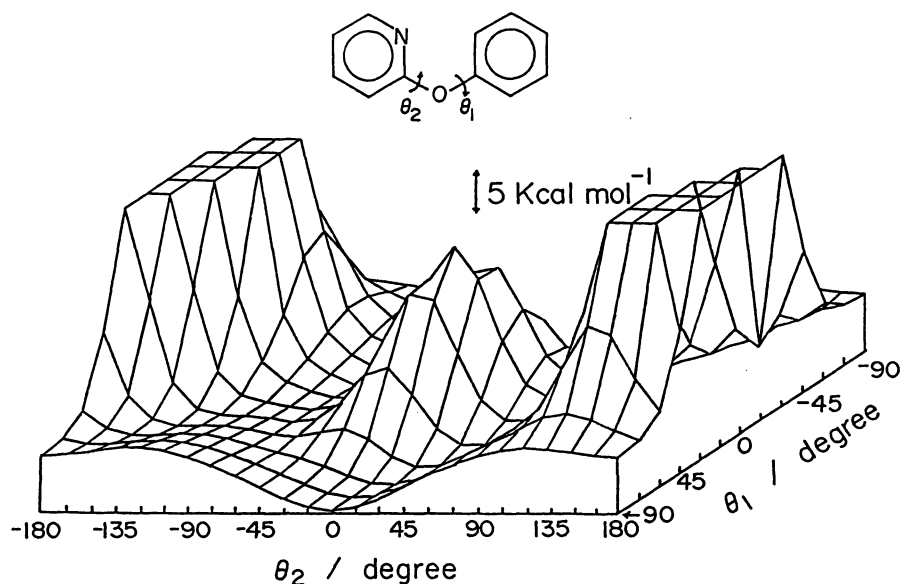


Fig. 6. STO-3G total energies of **2a** at 15° intervals of the θ_1 and θ_2 angles.

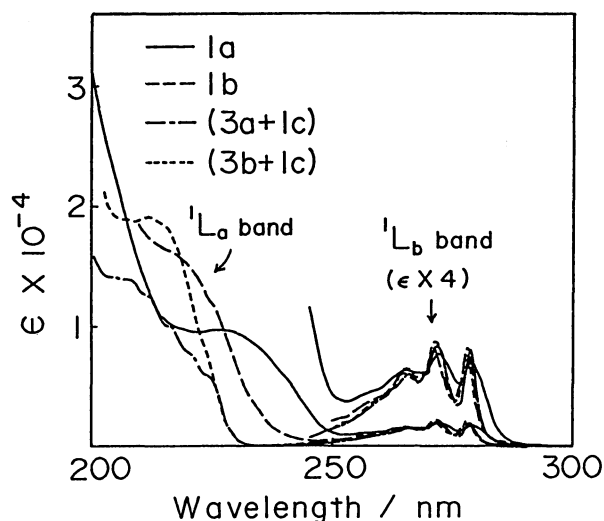


Fig. 7. Absorption spectra of **1a**, **1b**, and the composite spectra of (**3a+1c**) and (**3b+1c**) observed in heptane at room temperature.

other in the skew form of diphenyl ethers, the spectra of **1a** and **1b** should turn out to be similar to those of (**3a+1c**) and (**3b+1c**), respectively. Actually, this situation is almost satisfied for **1b**, as is shown in Fig. 7. A small difference in the transition energies between the 1L_a bands of **1b** and (**3b+1c**) may arise from the so-called through-space and through-bond interactions³⁰⁾ at the classically nonbonded position in **1b**. However, the 1L_a band of **1a** is observed at a longer wavelength with a smaller maximum intensity (see Fig. 7 and Table 1), compared with those of **1b**, (**3b+1c**), and (**3a+1c**). This would be ascribed to the fact that the conformation of **1a** is easily altered under the condition $\theta_1 + \theta_2 = 90^\circ$, as was predicted by STO-3G calculations. Table 2 summarizes the CNDO/S-CI calculation results for the structural alteration of **1a** in the range (0–90°) of θ_1 and θ_2 under the condition that $\theta_1 + \theta_2 = 90^\circ$. The parameters employed here result in a slightly larger transition

Table 2. CNDO/S-CI Calculation Results for the Conformational Change in **1a** and for **1c**

Compound (θ_1, θ_2)	Transition energy/eV	Oscillator strength	Assignment
1a (90°, 0°)	4.785	0.0055	1L_b
	4.815	0.0031	
	5.880	0.2287	1L_a
1a (75°, 15°)	4.780	0.0063	1L_b
	4.810	0.0031	
	5.817	0.2355	1L_a
	5.992	0.0160	
1a (60°, 30°)	4.770	0.0087	1L_b
	4.802	0.0028	
	5.727	0.2444	1L_a
	5.956	0.0275	
1a (45°, 45°)	4.763	0.0102	1L_b
	4.799	0.0027	
	5.691	0.2477	1L_a
	5.941	0.0327	
1c	4.818	0.0037	1L_b
	5.969	0.0627	1L_a

energy for these compounds than the experimental ones. Thus, the calculated transition energies should be valid compared with each conformer, rather than the absolute values. We can thus see that the conformational change in **1a** from skew to twist causes a sensitive shift of the calculated 1L_a transition energy to a longer wavelength. In turn, the dependence of the 1L_a band intensity (oscillator strength), which is quite large, on the conformational change is not very large. It would thus be difficult to assign the observed spectra to a fixed conformation of **1a**. The broad band of **1a** observed with a relatively small ϵ_{\max} should be explained in terms of the nonrigid conformation under the condition that $\theta_1 + \theta_2 \approx 90^\circ$, as predicted by the present STO-3G MO calculations.

Further evidence for the nonrigid conformation of **1a** has been given by the observation of a sharp, intensified

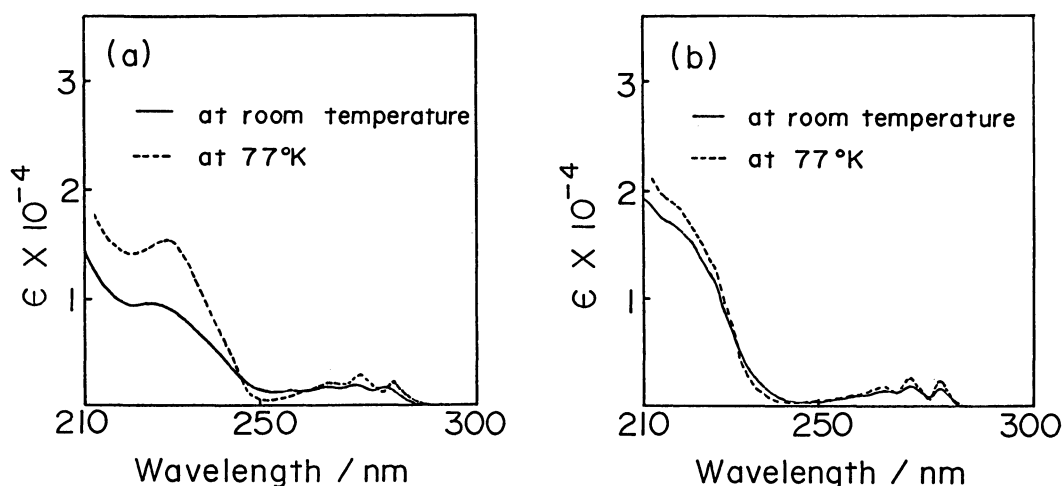


Fig. 8. Absorption spectra of **1a** (a) and **1b** (b) in an EPA solvent at 77 K.

and red-shifted 1L_a band at 77 K, compared to that at room temperature. The spectra of **1a** and **1b** recorded at 77 K are illustrated in Fig. 8, and their spectral data are summarized in Table 1. In general, the decrease in the temperature in spectral measurements makes the absorption band sharp, but does not affect either the absorption maximum or the integrated intensity.³¹⁾ Actually, the 1L_a and 1L_b bands of **1b** at 77 K indicate a tendency to become clear (Fig. 8b), and the spectral data are very close to those at room temperature, as can clearly be seen from Table 1. On the other hand, the 1L_a band of **1a** is remarkably intensified and red-shifted at 77 K (Fig. 8a and Table 1), the ϵ_{\max} being very close to that of **1b** with the skew conformation. These phenomena have been reasonably interpreted as indicating that **1a** is in a nonrigid conformation at room temperature and adopts a fixed one at lower temperature.

Electronic Spectra of 2-Phenoxypyridines. Figure 9

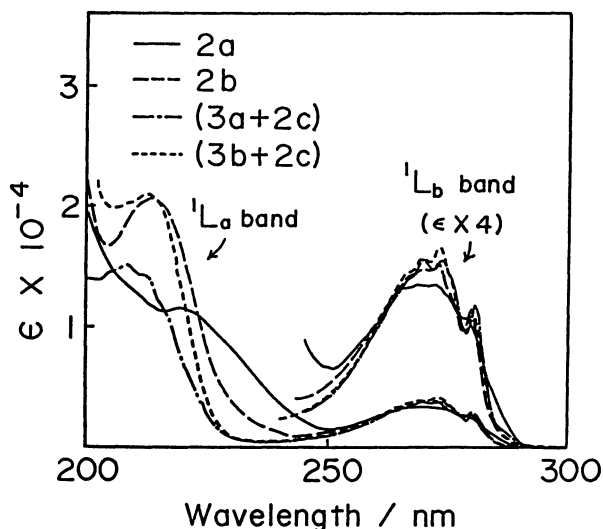


Fig. 9. Absorption spectra of **2a**, **2b**, and the composite spectra of (**3a**+**2c**) and (**3b**+**2c**) observed in hexane at room temperature.

depicts the UV spectra of **2a** and **2b**, together with the composite spectra of **3a** and **2c**, as well as those of **3b** and **2c**, being abbreviated as (**3a**+**2c**) and (**3b**+**2c**), respectively. The observed spectra of **2b** closely resemble the composite spectra of (**3b**+**2c**), except for a small difference in the 1L_a transition energy, which may be ascribed to the through-space and through-bond interactions in the skew form of **2b**. On the other hand, the 1L_a band of **2a** is broader than that of (**3a**+**2c**) and is considerably red-shifted. The spectral measurement at 77 K, however, did not provide any evidence for the preferable nonrigid conformation of **2a**, as shown in Table 1. A CNDO/S-CI calculation yielded interesting results concerning **2a**, as summarized in Table 3. The calculated spectra at $\theta_1=90^\circ$ and $\theta_2=0^\circ$ seem to correspond to the observed ones of **2b**, which preferentially adopt a skew conformation just like that of **1b**, as discussed hitherto in detail. As was discussed in the preceding chapter, **2a** is in a conformation that is slightly twisted from the symmetric skew form to an asymmetric one. This causes a remarkable change in the 1L_a spectral behavior. In the form of $\theta_1=75^\circ$ and $\theta_2=15^\circ$ the present calculations give three bands in the 1L_a region, whose oscillator strengths are almost of the same order and are somewhat smaller than in the 1L_a band predicted for the skew form of $\theta_1=90^\circ$ and $\theta_2=0^\circ$. These transitions are closely related to the 28th and 32nd occupied MO's (ϕ_{28} and ϕ_{32}); the 33rd—36th unoccupied MO's (ϕ_{33} — ϕ_{36}), as listed in Table 3. Both the electronic configurations ($\phi_{32} \rightarrow \phi_{33}$) and ($\phi_{32} \rightarrow \phi_{35}$) have a typical 1L_a character. The former also has a charge-transfer (CT) character from the phenyl ring to the pyridyl one. The ϕ_{28} of **2a** is a nonbonding orbital localized on the nitrogen atom of the pyridyl ring. The calculation results thus clearly indicate that the $\pi-\pi^*$ transitions in the 1L_a region occur as three substantial bands involving the interaction of the $n-\pi^*$ type configuration. This characteristic is brought about by a through-space interaction between the nitrogen lone-pair in the pyridyl ring and the π -system in the phenyl

Table 3. CNDO/S-CI Calculation Results for the Conformational Change in **2a** and **2c**

Compound (θ_1, θ_2)	Transition energy/eV	Configuration interaction/% ^{a)}	Oscillator strength	Assignment
2a ($90^\circ, 0^\circ$)	4.767	61.7(31/33), 22.2(29/34), 12.4(30/33)	0.0782	1L_b
	4.823	48.2(32/36), 35.2(30/35)	0.0026	
	5.953	50.4(32/35), 16.2(31/34)	0.2398	
2a ($75^\circ, 15^\circ$)	4.762	38.6(31/33), 20.0(29/34), 18.0(30/33), 17.3(32/33)	0.0770	1L_b
	4.819	23.0(32/36), 20.7(31/35), 18.1(32/35), 16.2(30/36)	0.0032	
	5.832	42.7(28/34), 22.4(32/34), 10.9(32/33)	0.0913	1L_a ^{b)}
	5.898	26.2(32/33), 24.8(32/35), 11.0(28/34)	0.0946	
	5.998	29.3(32/33), 23.1(32/35), 15.8(32/36)	0.0440	
2c	4.766	75.7(21/22), 23.8(20/23)	0.0767	1L_b
	6.061	75.9(21/23), 22.6(20/22)	0.0872	1L_a

a) For example, (31/33) means a singly excited configuration from the 31st filled MO (ϕ_{31}) to the 33rd unoccupied MO (ϕ_{33}). b) These bands are contributed from such electronic configurations as 1L_a and $n-\pi^*$ states, and a CT state from the phenyl to the pyridyl rings. See the text for details.

ring, and by the π -conjugation through the bridging oxygen atom. This is the reason why the 1L_a band of **2a** can be observed as a broader band at longer wavelengths than that of (**3a+2c**).

In conclusion, ab initio MO calculations and UV spectral analyses based on the CNDO/S-CI calculations suggest that **1a** prefers a nonrigid conformation whose dihedral angle of two phenyl rings is about 90° . Further evidence for the nonrigid conformation has been obtained from a spectral observation at 77 K. In the case of **2a**, however, that the conformer deviated somewhat from the symmetric skew conformation is the most reasonable interpretation. The broad 1L_a band of **2a** with smaller intensities is attributed to the interaction of the $n-\pi^*$ type configuration to the 1L_a states of the phenyl and pyridyl rings.

The authors thank the Computer Center, Institute for Molecular Science, Okazaki National Research Institutes for the use of the HITAC M-680H computer and the Library Program Gaussian 80.

References

- 1) M. Cory, D. D. McKee, J. Kagan, D. W. Henry, and J. A. Miller, *J. Am. Chem. Soc.*, **107**, 2528 (1985).
- 2) K. Fujikawa, K. Kondo, I. Yokomichi, F. Kimura, T. Haga, and R. Nishiyama, *Agric. Biol. Chem.*, **34**, 68 (1970).
- 3) P. A. Kollman, W. J. Murray, M. E. Nuss, E. C. Jorgensen, and S. Rothenberg, *J. Am. Chem. Soc.*, **95**, 8518 (1973).
- 4) P. A. Lehmann F., *J. Med. Chem.*, **15**, 404 (1972).
- 5) K. Higashi and C. P. Smyth, *J. Am. Chem. Soc.*, **82**, 4759 (1960).
- 6) S. P. N. van der Heijden, E. A. H. Griffith, W. D. Chandler, and B. E. Robertson, *Can. J. Chem.*, **53**, 2084 (1975); K. Gurtu, W. D. Chandler, and B. E. Robertson, *Can. J. Chem.*, **53**, 2093 (1975).
- 7) J. J. Bergman, E. A. H. Griffith, W. D. Chandler, and B. E. Robertson, *Can. J. Chem.*, **51**, 653 (1973).
- 8) P. A. Lehmann F., *Tetrahedron*, **30**, 719 (1974); D. M. McEachern B. and P. A. Lehmann F., *J. Mol. Struct.*, **11**, 127 (1972); P. A. Lehmann F. and E. Shefer, *Rev. Latinoam. Quim.*, **3**, 91 (1972).
- 9) K. Higashi, *Bull. Chem. Soc. Jpn.*, **35**, 692 (1962).
- 10) G. W. Buchanan, G. Montaudo, and P. Finocchiaro, *Can. J. Chem.*, **52**, 767 (1974).
- 11) I. Baraldi, E. Gallinella, and F. Momicchioli, *J. Chim. Phys.*, **83**, 653 (1986).
- 12) P. Dais, *Magn. Reson. Chem.*, **25**, 141 (1987).
- 13) T. Shaefer, G. H. Penner, C. Takeuchi, and P. Tseki, *Can. J. Chem.*, **66**, 1647 (1988).
- 14) J. Chao, M. A. Desando, D. L. Gourlay, D. E. Orr, and S. Walker, *J. Phys. Chem.*, **88**, 711 (1984).
- 15) F. Momicchioli, I. Baraldi, and M. C. Bruni, *Chem. Phys.*, **70**, 161 (1982).
- 16) D. Gust and K. Mislow, *J. Am. Chem. Soc.*, **95**, 1535 (1973).
- 17) D. Pitea and A. Ferrazza, *J. Mol. Struct.*, **92**, 141 (1983).
- 18) J. P. Bowen, V. V. Reddy, G. Patterson, Jr., and N. L. Allinger, *J. Org. Chem.*, **53**, 5471 (1988).
- 19) K. Higashi and S. Uyeo, *Bull. Chem. Soc. Jpn.*, **14**, 87 (1939), and the papers cited therein.
- 20) P. E. Weston and H. Adkins, *J. Am. Chem. Soc.*, **50**, 859 (1928).
- 21) A. Factor, H. Finkbeiner, R. A. Terusst, and D. M. White, *J. Org. Chem.*, **35**, 57 (1970).
- 22) M. Tomita, *J. Pharm. Soc. Jpn.*, **77**, 1024 (1957).
- 23) R. L. Ellis, G. Kuehnlenz, and H. H. Jaffé, *Theor. Chim. Acta*, **26**, 131 (1972); G. Kuehnlenz and H. H. Jaffé, *J. Chem. Phys.*, **58**, 2238 (1973); B. Tinland, *Mol. Phys.*, **16**, 413 (1969); N. O. Lipari and C. B. Duke, *J. Chem. Phys.*, **63**, 1748 (1975); C. B. Duke and N. O. Lipari, *J. Chem. Phys.*, **63**, 1758 (1975); P. Jacques, J. Faure, D. Chalvet, and H. H. Jaffé, *J. Phys. Chem.*, **85**, 473 (1981).
- 24) N. Mataga and K. Nishimoto, *Z. Phys. Chem.*, N. F. **13**, 140 (1957).
- 25) G. M. Anderson III, P. A. Kollman, L. N. Domelsmith, and K. N. Houk, *J. Am. Chem. Soc.*, **101**, 2344 (1978).
- 26) T. Shaefer, S. R. Salman, T. A. Wildman, and G. H. Penner, *Can. J. Chem.*, **63**, 782 (1985).
- 27) P. W. Jardon, E. H. Vickery, L. F. Pahler, N. Pourahmady, G. J. Mains, and E. J. Eisenbraun, *J. Org. Chem.*, **49**, 2130 (1984).
- 28) L. Radom, W. J. Hehre, J. A. Pople, G. L. Carlson, and W. G. Fateley, *J. Chem. Soc., Chem. Commun.*, **1972**, 308.
- 29) H. H. Jaffé and M. Orchin, "Theory and Application of Ultraviolet Spectroscopy," John Wiley and Sons, New York (1962).
- 30) T. Kobayashi, T. Kubota, and K. Ezumi, *J. Am. Chem. Soc.*, **105**, 2172 (1983).
- 31) M. Yamakawa, T. Kubota, K. Ezumi, and Y. Mizuno, *Spectrochim. Acta*, **30**, 2103 (1974).